THE AMERICAN MINERALOGIST, VOL. 50, NOVEMBER–DECEMBER, 1965

COALINGITE, A NEW MINERAL FROM THE NEW IDRIA SERPENTINITE, FRESNO AND SAN BENITO COUNTIES, CALIFORNIA

F. A. MUMPTON,[1] H. W. JAFFE[2] AND C. S. THOMPSON,[3]
Union Carbide Corporation, Mining and Metals Division, Tuxedo, New York.

ABSTRACT

A new mineral, coalingite, has been identified in the surface weathering zone of the New Idria serpentinite, Fresno and San Benito Counties, California. It occurs to a depth of 20–30 ft as soft, reddish-brown platelets, 0.1 to 0.2 mm in size, with resinous luster. Individual grains are contaminated with either chrysotile or a pyroaurite mineral, intimately intergrown with the coalingite, which has prevented the separation of absolutely pure fractions of this phase. Analyses of four concentrates and of a nearly-pure, hand-picked 500-mg sample have yielded the following empirical formula: $Mg_{10}Fe_2(CO_3)(OH)_{24}\cdot 2H_2O$.

Coalingite is uniaxial (−), with $\epsilon=1.563$ and $\omega=1.594$. It is pleochroic from golden-brown to colorless and is length slow. The measure density is 2.32 g/cc. *X*-ray diffraction studies clearly distinguish coalingite from closely related minerals such as brucite, pyroaurite, hydrotalcite and brugnatellite and suggest hexagonal symmetry. Differential thermal analyses of coalingite show three endothermic peaks at about 175°, 310° and 400° C. Thermal gravimetric analyses, *x*-ray diffraction and infrared absorption studies of heated specimens suggest that at about 120° C. a reversible dehydration takes place, accompanied by a rearrangement of the carbonate ions. At about 260° C. further rearrangement occurs without loss of CO_2, and at about 320° C. both CO_2 and hydroxyl water are evolved from the lattice, and a periclase phase is formed.

X-ray and petrographic studies of dense, dark green, unweathered portions of residual serpentinite, and of brown, friable, highly weathered counterparts indicate that coalingite forms *in situ* from pre-existing brucite, an important constituent of the serpentinite. Electron probe analyses have shown the presence of up to 18 weight per cent iron in brucite from this body, sufficient to form coalingite directly without the introduction of iron from an external source. These data, combined with the observed transformation of brucite-rich specimens to coalingite in the laboratory after beng exposed to the atmosphere for several months, strongly indicate that coalingite is formed by the oxidation and carbonation of iron-rich brucite in the surface weathering zone of the serpentinite. Artinite and hydromagnesite are also found in the weathering zone, but are decidedly later and probably precipitated directly from magnesium-rich ground waters.

The name coalingite (kōl-ing-gīt) is proposed for this new mineral referring to the nearby town of Coalinga, California. It is likely that many of the so-called "ferrobrucites," inadequately described in the literature, are actually coalingite or coalingite-rich mixtures.

INTRODUCTION

Although the New Idria serpentinite body has been recognized for over one hundred years and has been described in some detail by several au-

[1] Present address: U. S. Geological Survey, Menlo Park, California.

[2] Present address: Department of Geology, University of Massachusetts, Amherst, Mass.

[3] Present address: Department of Mineralogy, University of Utah, Salt Lake City, Utah.

thors, including Eckel and Myers (1946) and Coleman (1957), it was not until 1958 that the potential value of the short-fiber asbestos present in certain areas of this mass was recognized. Since that time, however, the New Idria serpentinite has been thoroughly explored by several mining companies and more than 300 claims have been filed on this deposit within the last six years. During this period the town of Coalinga, California, became the headquarters for the asbestos exploration activities, hence the deposit became known as the Coalinga asbestos deposit.

The New Idria serpentinite is located in Fresno and San Benito Counties, California, about 35 miles northwest of Coalinga, and covers an area about 5 by 17 miles in size. The intrusive serpentinite lies almost directly along the axis of the Coalinga anticline, where it forms resistant ridges surrounded by lower, rounded hills. Both the serpentinite and the asbestos deposits located in the southeastern third of the body are composed almost entirely of members of the serpentine group of minerals, primarily chrysotile. Minor quantities of brucite and magnetite are also present, as are traces of chromite, calcite and uvarovite garnet. One of the most striking features of the deposit is the oxidized appearance of the asbestos ore at the surface. Fresh, unaltered ore is gray-green in color and whitens upon standing. At the surface, however, the ore is reddish-brown, obviously due to the presence of oxidized iron.

During the mineralogical examination of samples from the surface weathering zone, the presence of small (0.1 to 0.2 mm) mica-like platelets of a brown, translucent mineral was noted. The optical and *x*-ray diffraction properties of this phase could not be matched with those of any known mineral and, therefore, the existence of a new mineral species was postulated. A detailed examination of this material was made, the results of which are presented here, confirming this hypothesis. The name coalingite (kōl-inǵ-gīt) is proposed for this new mineral referring to the nearby town of Coalinga, California. This mineral has been approved by the Commission on New Minerals, International Mineralogical Association.

Geologic Occurrence

The Coalinga asbestos deposit bears little resemblance to most of the well-known asbestos deposits of the world, since individual fibers of chrysotile are nowhere visible to the naked eye. It resembles a gigantic pile of highly sheared and pulverized serpentine, having little strength or coherence. Scattered throughout the body, however, are hard, competent masses of residual serpentinite, varying in size from fractions of an inch to boxcar dimensions, which have apparently withstood the intense deformation and today stand out as resistant outcrops and "boulders," sur-

rounded by much softer, friable asbestos material. Although it is essentially absent from the ore at depth, coalingite is abundant in the surface weathering zone of the serpentinite. The brown-colored weathering zone normally extends to a depth of about twenty or thirty feet and covers the entire body. A closer examination reveals that within this zone, the residual serpentinite fragments and "boulders" appear to be highly oxidized, while the soft, friable asbestos material surrounding them is relatively unchanged and only slightly discolored. Serpentinite "boulders" close to the surface are highly oxidized and extremely friable, disintegrating readily upon standing, into a soft, brown powder.

A member of the hydrotalcite-pyroaurite group is also abundant, and is intimately associated with both coalingite and serpentine in many samples. Neither mineral has heretofore been recognized from this deposit. The hydrous magnesium carbonates, artinite and hydromagnesite, are also abundant in the surface weathering zone. Artinite occurs as radiating white needles, usually a few millimeters in length, and is commonly found as surface coatings on residual serpentine fragments. Hydromagnesite occurs as small, white concretions, varying in size from about 1/16″ to 1″. Areas have been noted in which hydromagnesite makes up about 10% to 25% of the surface ore, scattered throughout the green asbestos matrix. Soft, chalk-like hydromagnesite has also been found in veins up to an inch thick, associated with fractures and cavities in the residual serpentinite masses. Both of these phases definitely appear to be secondary, in that they have probably precipitated directly from the Mg-rich, CO_2-rich ground waters which saturate the upper part of the ore.

Hand specimens of coalingite are reddish-brown and have a resinous luster. Although these masses appear to be almost pure coalingite, they usually contain no more than about 25–50% of this mineral, the remainder being mainly serpentine. Individual plates or stacks of plates of coalingite can be seen, although these are almost invariably contaminated by intimately intergrown chrysotile and/or hydrotalcite. Heavy liquid, magnetic, sedimentation and other purification techniques all yielded high-grade concentrates, but none produced a *pure* end product. A 500 milligram pure sample was prepared by Mr. P. Pezzella who tediously hand-picked 200-mesh size grains from some of these concentrates under the binocular microscope. Even this sample proved to be contaminated by intimately intergrown laths of hydrotalcite, as shown by x-ray diffraction and microscopic examinations.

Individual grains of coalingite are quite soft, with an estimated hardness of about 1 or 2, and are deep, reddish-brown in color. Coalingite forms plates and resembles phlogopite both in direct and transmitted light. Equant grains, however, are also abundant in most samples.

TABLE I. *X*-RAY DIFFRACTION DATA[1] FOR COALINGITE AND RELATED MINERALS

Coalingite $Mg_{10}Fe_2CO_3(OH)_{24}\cdot 2H_2O$		"Coalingite-K" (?)		Hydrotalcite $Mg_6Al_2CO_3(OH)_{16}\cdot 4H_2O$		Sjögrenite[2] $Mg_6Fe_2CO_3(OH)_{16}\cdot 4H_2O$		Pyroaurite[3] $Mg_6Fe_2CO_3(OH)_{16}\cdot 4H_2O$		Pyroaurite[4] $Mg_6Fe_2CO_3(OH)_{16}\cdot 4H_2O$		Brugnatellite[5] $Mg_6FeCO_3(OH)_{12}\cdot 4H_2O$		Brucite[6] $Mg(OH)_2$		
New Idria Serp.		New Idria Serp.		Snarum, Norway		Långban, Sweden		Canada (?)		Ural Mts., USSR		Val Malenco, Italy		Synthetic		
d	I/I_0	d	I/I_0	d	I/I_0	d	I/I_0	d	I/I_0	d	I/I_0	d	I/I_0	d	I/I_0	(hkl)
13.4	4B	18.8	3B	7.83	10	7.78	10	7.6	10	7.709	VS	8.02	6	4.77	90	001
6.05	5	5.72	5	—	—	—	—	—	—	6.388	W	—	—	2.725	6	100
4.75	1	4.75	1	—	—	—	—	4.8	1*	—	—	4.757	8*	2.365	100	101
4.20	8	4.38	10	3.92	9	3.90	6	3.89	7	4.154	M	3.975	6	1.794	56	102
2.67	3	2.70	4	—	—	—	—	—	—	3.817	S	—	—	1.573	36	110
2.62	½	2.61	½	—	—	3.24	<1	—	—	—	—	—	—	1.494	18	111
2.52	1B	2.45	½	—	—	3.08	<1	—	—	—	—	—	—	1.373	16	103
2.34	10	2.36	10	—	—	2.86	<1	—	—	2.901	W	—	—	1.363	2	200
—	—	2.21	1	2.62	6	2.65	4	2.62	4	2.625	S	2.676	6	1.310	11	201
1.884	3	1.88	4	—	—	2.54	5	—	—	—	—	—	—	1.192	2	004
1.767	3	1.79	6	2.31	6	2.39	3	2.33	4	2.334	VS	2.361	10*	1.183	9	202
1.712	3	1.75	6	—	—	2.21	5	—	—	—	—	—	—	1.118	1	113
1.558	5	1.57	9	1.97	8	2.04	2	1.981	5	1.974	M	1.992	6	1.092	3	104
—	—	1.54	½	—	—	1.87	5	—	—	—	—	—	—	1.034	5	203
1.509	1	1.51	1	1.755	3	—	—	1.763	1	1.760	M	1.786	8	1.030	1	210
1.462	1	1.48	3	1.662	3	1.57	1	1.670	1	—	—	—	—			
1.430	½	1.43	½	1.535	4	1.55	2	1.556	2	1.560	M	1.571				
—	—	1.40	½	1.506	5	1.52	2	1.526	2	1.527	M					
1.313	½	1.34	3	—	—	—	—	1.497	1	—	—					
1.298	1	1.31	3	1.427	2	1.44	1	1.448	1	—	—					
—	—	1.25	1	—	—	1.35	1	—	—	1.346	VW					
—	—	1.23	1	1.322	1	1.33	<1	1.335	1	—	—					
0.998	1B	—	—	1.302	1	1.29	<1	1.292	2	1.295	W					
				1.282	3	1.27	<1	—	—							
				1.212	2	1.19	<1	1.223	1							
				—	—	1.17	<1									
				0.980	1											

* Brucite?

[1] Data are taken from film patterns, since the preparation techniques inherent in the diffractometer method yield highly oriented specimens.

[2] New York Museum of Natural History sample number 19820, labeled pyroaurite. This is definitely the hexagonal polymorph, sjögrenite as defined by Frondel (1941). Sample supplied by Brian Mason.

[3] Data from Sabina and Trail (1960). Locality unknown; may be the pyroaurite described by Ellsworth (1939).

[4] Data from Ginzburg and Rukavishnikova (1951).

[5] Data from Fenoglio (1938). Note the similarity between this pattern and that of pyroaurite. Frondel (1941) examined a brugnatellite specimen from Val Malenco and identified it as mainly pyroaurite.

[6] Data from Swanson *et al.* (1956), p. 30, Synthetic $Mg(OH)_2$.

X-RAY DIFFRACTION PROPERTIES

The unique character of coalingite was first recognized by means of its distinctive *x*-ray diffraction pattern. The powder diffraction data of a hand-picked sample of coalingite are presented in Table I, along with those of several related phases. Most studies were made with a Norelco High Angle Diffractometer or a 114.6-mm diameter powder camera, using Ni-filtered Cu Kα radiation. From these data and from the tracings shown in Fig. 1, the *x*-ray diffraction pattern of coalingite can easily be distinguished from those of the hydrotalcite-pyroaurite group, and from

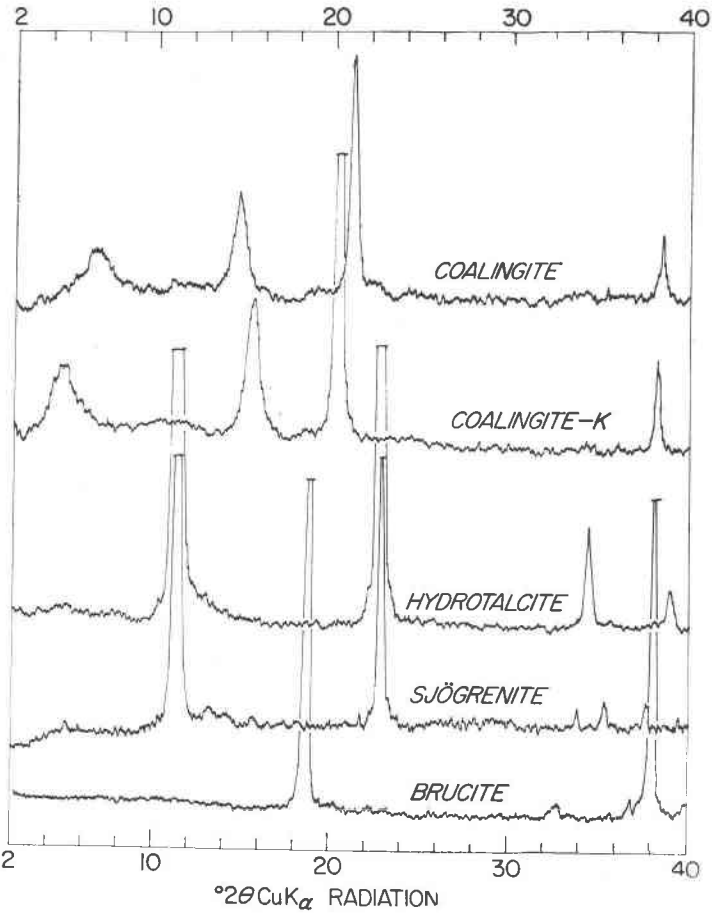

FIG. 1. *X*-ray diffraction tracings of coalingite and related minerals. Hydrotalcite from Snarum, Norway; sjögrenite from Långban, Sweden, New York Museum of Natural History No. 19820; brucite from Lodi, Nevada.

that of brugnatellite. Although minor variations in the optical properties of coalingite have been noted (*vide infra*) no differences in the x-ray patterns of many samples of coalingite could be detected.

Preliminary single crystal studies by Mrs. G. Faulring have suggested hexagonal symmetry for coalingite. Attempts at indexing the powder diffraction pattern, however, have been largely unsuccessful, due to the presence of both sharp and diffuse reflections. These data indicate that the specimen examined may be either a faulted single phase or an intimate mixture of two phases having the same orientation. All attempts at separating coalingite into separate phases have failed and all products give rise to x-ray diffraction patterns having the same relative peak intensities. In addition, chemical analyses of several different concentrates of coalingite each yield essentially the same empirical formula.

A material closely related to coalingite was found by Mr. R. J. Kronkhyte during the processing of the Coalinga asbestos ore and has been temporarily designated as "coalingite-K." The x-ray pattern of "coalingite-K" listed in Table I and shown in Fig. 1 is similar to that of coalingite, although the peaks are shifted. Although the lack of material has prevented a chemical analysis of this material, "coalingite-K" probably represents a compositional variation of "normal" coalingite. To date "coalingite-K" has been found in only one small hand specimen.

X-ray diffraction studies of impure concentrates of the hydrotalcite-pyroaurite material indicate that this phase is the rhombohedral polymorph of this group, that is, either hydrotalcite or pyroaurite, rather than manasseite or sjögrenite. The cell dimensions of the aluminum end-member, hydrotalcite, and the iron end-member, pyroaurite, are too close for an unequivocal identification of this phase by the x-ray diffraction techniques used.

Optical Properties

The optical properties of coalingite were determined by ordinary immersion techniques and are listed in Table II, along with data for other related phases. Coalingite is readily identified optically by its indices of refraction which are slightly higher than those of minerals with which it might easily be confused, such as pyroaurite, sjögrenite, brugnatellite, etc. Under the microscope it resembles phlogopite at first glance, in that it is platy, is markedly pleochroic from golden brown (ω) to colorless (ϵ), and is uniaxial negative. The optical properties of coalingite are not dissimilar from those reported in the literature for various "ferrobrucites," although the latter materials have never been completely characterized and cannot be considered as valid mineral species (see, for example, Abovyan, 1957; Meixner, 1937). The optical properties of coalingite are

TABLE II. OPTICAL CONSTANTS AND SPECIFIC GRAVITY OF COALINGITE AND RELATED MINERALS

	Coalingite $Mg_{10}Fe_2CO_3(OH)_{24}\cdot 2H_2O$	"Coalingite-K" (?)	Brucite[1] $Mg(OH)_2$	Pyroaurite $Mg_6Fe_2CO_3(OH)_{16}\cdot 4H_2O$			Hydrotalcite[2] $Mg_6Al_2CO_3(OH)_{16}\cdot 4H_2O$	Brugnatellite[2] $Mg_6FeCO_3(OH)_{12}\cdot 4H_2O$
					(*a*)[3]	(*b*)		
ω	1.594	(β, γ) 1.579	1.559	1.564[2]	1.584	1.603	1.511	1.540
ϵ	1.563	(α) 1.564	1.580	1.543	1.552	1.573	1.495	1.510
ω-ϵ	0.031	0.015	0.021	0.021	0.032	0.030	0.016	0.030
Sign	(−)	(−)	(+)	(−)	(−)	(−)	(−)	(−)
(2V)		~0°–10°						
S.G. (g/cc)	2.33	~2.25	2.4	2.12			2.06	2.14

[1] Optical and density data from Larsen and Berman (1934).

[2] Optical and density data from Frondel (1941)

[3] Optical data from Ginzburg and Rukavishnikova (1951) for (a) pale brown and (b) dark brown platelets.

also similar to those reported by Ginzburg and Rukavishnikova (1951) for several types of pyroaurite from the Urals. The indices of refraction of these materials, however, are considerably higher than those reported for most pyroaurites, and the *x*-ray diffraction pattern, chemical analyses and DTA diagrams reported by these authors allow a clear distinction to be made between coalingite and these particular types of pyroaurite.

In transmitted light most coalingite grains occur as deep golden-brown, non-pleochroic plates that lie on or near a prominent parting plane or cleavage (basal?). Under crossed polars, many of these plates are sensibly isotropic and yield uniaxial negative interference figures. Some, however, which are visibly strained and exhibit undulant extinctions, yield anomalous biaxial negative figures with axial angles varying from 5° to 20°. Elongate grains oriented normal to the plates show marked pleochroism, from deep golden brown to colorless, with absorption $\omega > \epsilon$, moderately strong birefringence and length slow orientation. The indices of refraction of coalingite show a moderate amount of variation in different concentrates, within a single concentrate, and in some instances, within a single 200 mesh-size grain which is otherwise in optical continuity. The indices of refraction determined on different grains of coalingite were found to vary within the following limits:

ω	1.588	1.592	1.594	1.606	all $\pm$ 0.002
ϵ	1.560	1.564	1.563	1.575	
ω-ϵ	0.028	0.028	0.031	00031	

Although the indices of individual grains vary within narrow limits, the maximum birefringence and absorption remain essentially constant. Elongate grains, showing the maximum birefringence are commonly striated parallel to the elongation (the slow vibration direction), suggesting that the observed variations in the indices of refraction result from the alternate stacking of layers or plates of slightly different composition. Since the compositional variation does not appear to be of sufficient magnitude to produce a measurable shift in the *x*-ray diffraction pattern of different samples of coalingite, the attendant index of refraction spread is probably due to slight variations in the degree of hydration, rather than to changes in the Mg:Fe ratios, or in the CO_3 orientation, which might be expected to modify the total birefringence as well as the values of the indices.

In the case of "coalingite-K," marked changes in both the indices of refraction and the total birefringence have been noted (Table II). All grains of "coalingite-K" appear to be strained and show biaxial negative interference figures, with axial angles varying from near 0° to 10°, suggesting that this phase is only pseudo-hexagonal, whereas coalingite proper may be hexagonal.

Specific Gravity

The specific gravity of coalingite was determined on grains averaging between 150 and 200 mesh in size, using the heavy liquid technique. Two independent determinations yielded the values 2.32 and 2.33 g/cc at 24° C. for the specific gravity of coalingite. These data are compared with the densities of related minerals in Table II. The slightly lower density of "coalingite-K" (~2.25 g/cc) suggests a somewhat lower iron content for this variety, compared with coalingite proper. This value was determined on single grains on a Berman balance.

Chemical Composition

As mentioned above, the separation of pure coalingite has been a near-impossible task, and even the most highly purified, hand-picked concentrates were still found to be contaminated with intimately intergrown hydrotalcite and/or chrysotile. Four concentrates, however, each containing a different amount of chrysotile impurity and with a minimum of hydrotalcite, were prepared by heavy media and magnetic separation techniques. Chemical analyses of these samples and of the hand-picked, "pure" sample are listed in Table III along with rationalized mole percentages calculated from these data. These calculations were carried out by deducting from each analysis the amount of chrysotile that was estimated from the silica content of the analysis. Calcite was also subtracted in the same manner, using the CaO value from the analysis. The data were then rationalized into atomic ratios and the following formula obtained for coalingite: $Mg_{10}Fe_2(CO_3)(OH)_{24}\cdot 2H_2O$. The mole percentages of all analyses and of the proposed empirical formula are also listed in Table III.

Coalingite is chemically similar to the so-called "ferrobrucites" in the literature and it is not unlikely that many of these substances are actually coalingite or coalingite-rich mixtures. More comprehensive *x*-ray diffraction and optical studies of "ferrobrucite" materials are needed to provide reliable identifications.

Infrared Absorption Properties

Infrared absorption patterns of coalingite and several related minerals were recorded using a Perkin-Elmer Model 221, double-beam, infrared spectrophotometer, with rock salt optics. The KBr pellet technique was used in which the sample concentration was held constant at 0.25%. From the patterns listed in Fig. 2, it is apparent that the infrared spectrum of coalingite closely resembles those of members of the hydrotalcite-pyroaurite group, and is considerably different from those of other hydrous magnesium carbonates, such as artinite and hydromagnesite. The coalingite pattern is characterized by the presence of the stretching

TABLE III. CHEMICAL ANALYSES OF COALINGITE CONCENTRATES[1]

Wt.–%	487-20-1 Concentrate	487-20-2 Concentrate	487-20-3 Concentrate	487-20-4 Concentrate	487-27-1 "Pure" Fraction[2]
SiO_2	11.13	4.82	6.17	8.74	1.7
MgO	45.49	46.43	45.46	45.54	46.1
FeO	0.11	0.05	0.07	0.05	n.d.
Fe_2O_3	14.87	16.97	16.40	14.89	18.3
CaO	0.64	0.38	0.57	0.53	0.5
CO_2	3.03	3.87	3.61	3.39	4.8
$H_2O(+)$	24.66	27.53	27.77	26.90	28.8
Total	99.93	100.05	100.05	100.04	100.7

Rationalized Mole Per Cents

	487-20-1 Concentrate	487-20-2 Concentrate	487-20-3 Concentrate	487-20-4 Concentrate	(Average 1–4)	487-27-1 "Purified"	Theoretical $Mg_{10}Fe_2CO_3(OH)_{24}\cdot 2H_2O$ Mole %	Theoretical $Mg_{10}Fe_2CO_3(OH)_{24}\cdot 2H_2O$ Wt. %
MgO	39.21	38.78	38.36	37.86	(38.55)	38.56	38.5	46.9
Fe_2O_3	4.09	3.92	3.85	3.73	(3.98)	3.99	3.9	18.6
CO_2	2.62	3.04	2.75	2.79	(3.80)	3.51	3.9	5.1
H_2O	54.08	54.26	55.04	55.62	(54.75)	53.94	53.7	4.2 (H_2O) 25.2 (OH)

Atomic Ratios
(Cations on the basis of 29 oxygens)

Mg	10.31	10.16	9.93	9.99	10.08	10	
Fe^{3+}	2.16	2.06	2.05	1.97	2.08	2	
C	0.73	0.81	0.75	0.76	0.92	1	
H	28.02	28.28	29.02	29.06	27.85	28	

[1] All concentrates contain small amounts of chrysotile and a hydrotalcite-pyroaurite mineral. An analysis of chrysotile similar to this impurity gave: SiO_2 41.42, Fe_2O_3 2.05, FeO 1.61, CaO 0.54, MgO 40.62, H_2O 13.66 wt. %.

[2] Includes 0.4% MnO_2, 0.05% Al_2O_3. Sample totaled less than 0.500 grams, hand-picked from 200 mesh-size material.

bands of water in the region 2.5 to 3.0 microns and by strong absorptions at about 6.5 and 7.1 microns, corresponding to carbonate stretching vibrations. Minor Si-O bands are also present in several of the patterns shown in Fig. 2 but are due to the presence of admixed serpentine.

THERMAL STABILITY

The thermal stability of coalingite has been investigated by means of differential thermal analyses (DTA), thermal gravimetry (TGA), and static heating experiments, the results of which are shown in Figs. 3 to 5, and tabulated in Table IV. The TGA pattern in Fig. 4 was obtained using a Stanton Thermobalance. All weight losses must take into account the presence of about 15–20% chrysotile in the sample examined. Thus a weight loss of 21% recalculated to approximately 25%.

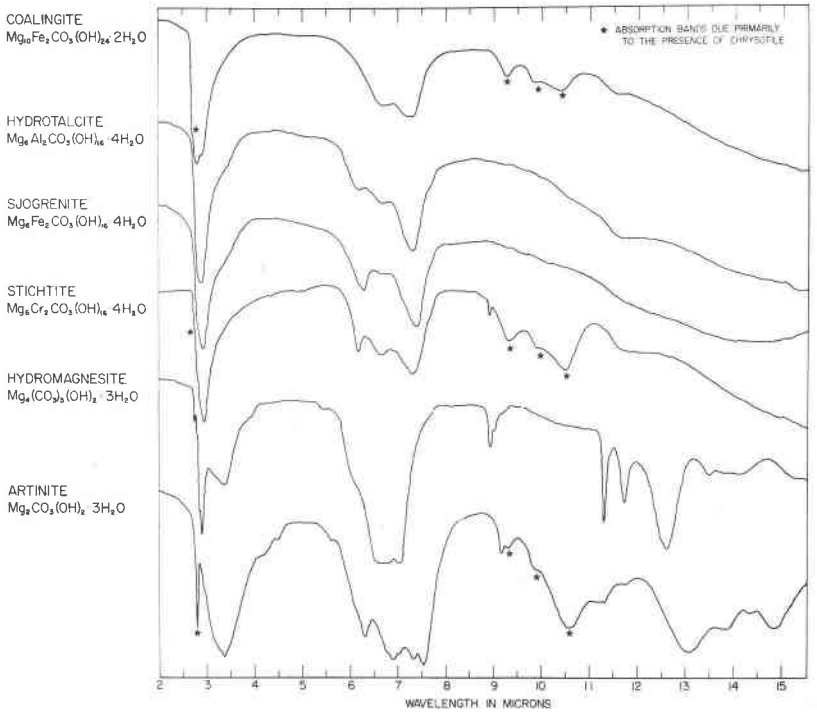

FIG. 2. Infrared spectra of coalingite and related minerals.

Three separate endotherms can be observed in the DTA pattern of coalingite, not including the weak reaction peaks in the region 600°–800° C., which are due to the presence of admixed chrysotile in the sample. From a consideration of the proposed formula for coalingite, $Mg_{10}Fe_2(CO_3)(OH)_{24}\cdot 2H_2O$, and the thermal gravimetric data shown in Fig. 4, the endotherm at about 175°–180° C. corresponds to the loss of the two waters of crystallization from the coalingite structure. The second endotherm at about 310°–315° C. was first thought to be due to the loss of carbon dioxide from the structure, but the results of the static heating experiments discussed below indicated that this peak corresponds to a structural transition, rather than to a weight-loss reaction of any kind. The absence of a break in the TGA curve in this temperature region also supports this contention. The very strong endotherm at about 400°–405° C. must therefore correspond to the loss of both CO_2 and OH water from the structure.

The DTA pattern of hydrotalcite from Snarum, Norway, also shown in Fig. 3, exhibits endotherms similar to those of coalingite, but at slightly different temperatures and with different magnitudes, suggesting that

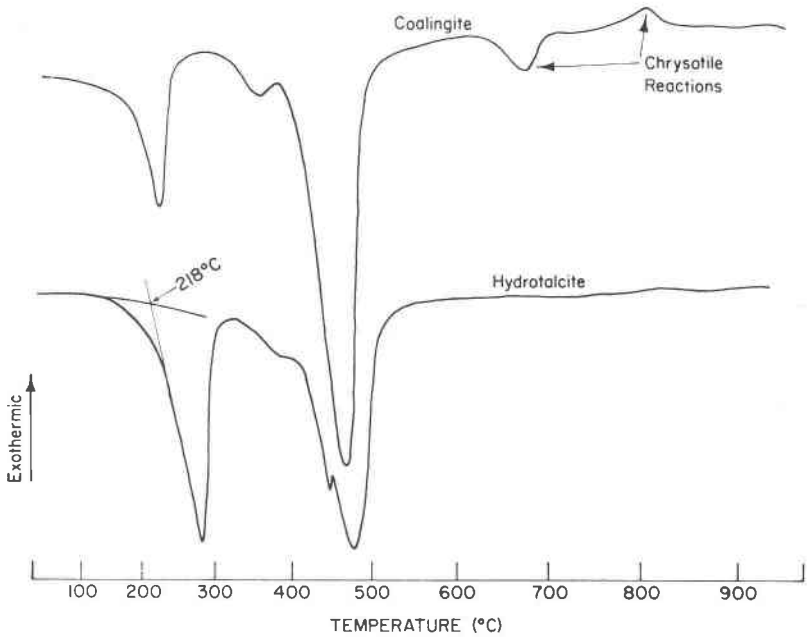

FIG. 3. Differential thermal analysis patterns of coalingite and hydrotalcite.

minerals of the hydrotalcite-pyroaurite group behave in a similar manner when heated. The evolution of CO_2 from the hydrotalcite lattice may well account for the sharp peak on the side of the major endotherm, which in coalingite, is merely not resolved.

In order to characterize more completely the phases formed by the thermal decomposition of coalingite, as well as to verify the above assignments of endotherms, a number of static heating experiments were carried out, the results of which are listed in Table IV. Approximately 500 mg of "purified" coalingite, containing about 10% chrysotile and trace quantities of brucite and hydrotalcite, were heated statically in a small furnace. At the end of each heating period small samples were examined by means of infrared absorption techniques or by film *x*-ray diffraction methods. Frequently, samples which had dehydrated were found to rehydrate upon exposure to the atmosphere in a matter of hours. In this case, additional *x*-ray and/or I.R. studies of the rehydrated material were also made.

From the results listed in Table IV, it can be seen that coalingite decomposes in three distinct steps, corresponding to the formation of several structurally unique phases. Natural coalingite is stable in air to about 120° C. whereupon it loses its waters of crystallization. At this temper-

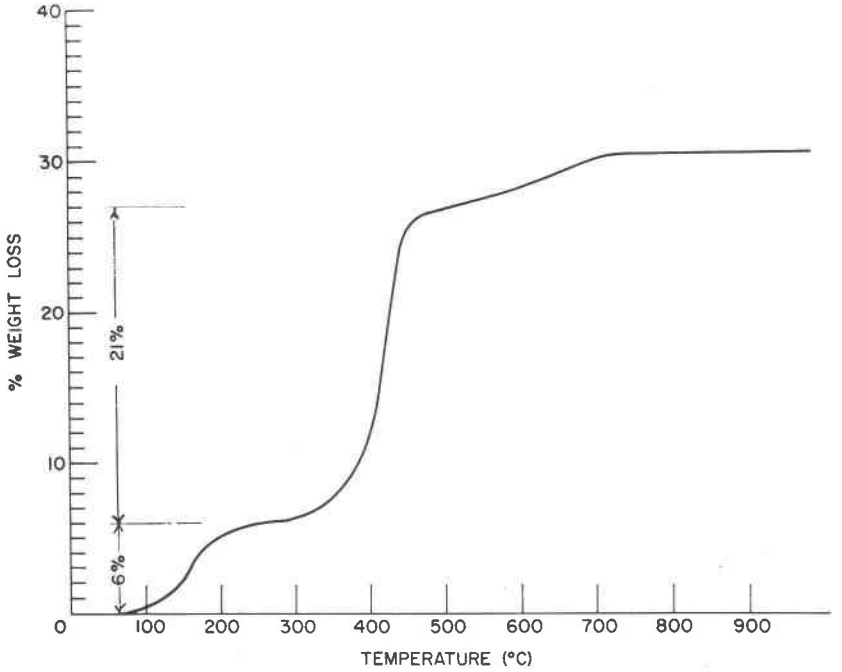

FIG. 4. Thermal gravimetric analysis of a colaingite-rich concentrate (containing about 15% chrysotile).

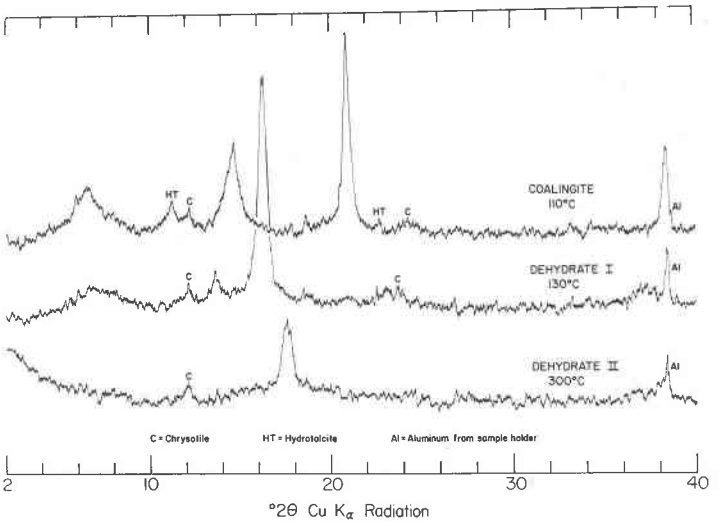

FIG. 5. *X*-ray diffraction parterns of coalingite heated to various temperatures.

TABLE IV. RESULTS OF STATIC HEATING EXPERIMENTS ON COALINGITE

Sample	Temperature ° C.	Time hours	Coalingite phases present[1]	
			x-ray diffraction	Infrared absorption
487-74-1	25	—	Coalingite	Coalingite
487-74-2	110	4	Coalingite	Coalingite
487-74-3	130	64	Coalingite[3]	Dehydrate I
487-74-4	150	20	Coalingite[3]	Dehydrate I
487-74-5	165	16	Dehydrate I	Dehydrate I
487-74-6	Rewet[2]	—	Coalingite	Dehydrate I
487-74-7	187	16	Dehydrate I	Dehydrate I
487-74-8	Rewet[2]	—	Coalingite	Not Determined
487-74-9	220	17	Dehydrate I	Dehydrate I
487-74-10	Rewet[2]	—	Coalingite	Not Determined
487-74-11	247	16	Dehydrate I	Dehydrate I
487-74-12	Rewet[2]	—	Coalingite	Not Determined
487-74-13	265–270	16	Dehydrate II	Dehydrate I
487-74-14	Rewet	—	Dehydrate II	Dehydrate I
487-74-15	285–290	18	Dehydrate II	Dehydrate II
487-74-16	315	6	Dehydrate II	Dehydrate II
487-74-17	335–340	66	Periclase	Periclase
487-74-18	360	16	Periclase	Periclase
487-74-19	395–400	16	Periclase	Periclase
487-74-20	440–445	18	Periclase	Periclase
487-74-21	495	18	Periclase	Periclase

[1] Admixed chrysotile was present in all samples. *X*-ray patterns of all phases are listed in Table V.

[2] "Rewet" samples represent the rehydrated counterparts of the previous sample. This was accomplished by adding several drops of water to both the *x*-ray mount and the material in the crucible and allowing them to dry at slightly above room temperature.

[3] The anomalous existence of coalingite above 120° C. is discussed in the text.

ature a phase designated as dehydrate I is formed, which has an *x*-ray diffraction pattern distinct from that of coalingite or any other known phase (Table V and Fig. 5). From infrared data there appears to be no loss of CO_2 accompanying this reaction, although a slight rearrangement of the carbonate ion in the lattice is indicated from shifts in the positions of the two main carbonate bands in the I. R. spectrum. The first endotherm of the DTA pattern and the initial weight loss shown on the TGA pattern verify a reaction of this type in this temperature region.

If the dehydrate I phase is rewet, or allowed to stand exposed to the atmosphere for several hours, the dehydration reaction is reversed and the sample rehydrates, yielding a material having an *x*-ray pattern identical with the original coalingite starting material. The dehydration-re-

TABLE V. *X*-RAY DIFFRACTION PATTERNS OF COALINGITE AND DEHYDRATED PRODUCTS

Coalingite[1]		487-74-9 Dehydrate I[2]		487-74-2A Dehydrate II[1]		487-74-22 Periclase[1]	
d	I/I_0	d	I/I_0	d	I/I_0	d	I/I_0
13.4	4B	6.46	2	5.00	5		
6.05	5			2.70	1		
4.75	1	5.44	10	2.37	9	2.43	1
4.20	8	3.80	2	2.12	<1	2.10	10
2.67	3	2.40	2	1.79	<1		
2.62	½	1.73	2	1.55	5		
2.52	1B	1.56	2	1.49	<1	1.49	7
2.34	10			1.31	<1	1.27	<1
1.884	3					1.22	1
1.767	3						
1.712	3						
1.558	5						
1.509	1						
1.462	1						
1.430	½						
1.313	½						
1.298	1						
0.998	1B						

[1] Measured from film.

[2] Measured from diffractometer tracing.

hydration reaction has been accomplished several times with the exact same sample of coalingite at about 120° C. Upon rehydration, the carbonate infrared absorption bands do not revert to their original positions indicating that the carbonate ions, once re-oriented remain unchanged when the sample is rehydrated. It should be pointed out that in many cases the *x*-ray diffraction pattern of coalingite changes to that of the dehydrate I phase at 120° C. *only* after the sample has been preheated at a higher temperature. The sample used in this experiment required a preheating at 165° C. (Table IV); others failed to transform until they had been heated to nearly 200° C. In all cases, however, once the transformation had taken place, all samples then reacted rapidly and reversibly at 120° C.; the carbonate absorptions changed position immediately at 120° C., even when the *x*-ray diffraction pattern remained that of normal coalingite. The explanation for this behavior is still under investigation.

The dehydrate I phase is stable to about 255°–275° C., where it transforms into another phase, dehydrate II. The dehydrate II phase is also characterized by a unique *x*-ray diffraction pattern, as listed in Table V and shown in Fig. 5. Above 275° C. a further rearrangement of the

carbonate ions in the lattice is indicated by infrared absorption data. This reaction is not reversible and apparently represents a structural transition which is *not* accomplished by a loss of either CO_2 or water. No weight loss in this temperature region is indicated from either the TGA pattern or the infrared absorption spectra and therefore the small endotherm shown in the DTA pattern must correspond to a transition, rather than to a loss of volatile constituents.

Dehydrate II is stable only over a narrow temperature range and decomposes to periclase at approximately 320° C. No attempt has been made to characterize completely the oxide product and undoubtedly a

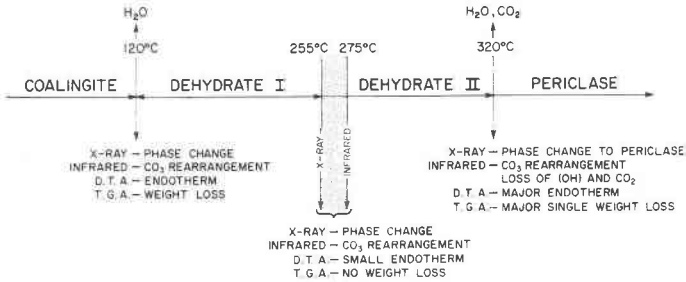

FIG. 6. Thermal decomposition schematic for coalingite.

small amount of iron is present in the periclase lattice. From the infrared data a third rearrangement of the carbonate ions is indicated and although a marked decrease in the absorption values for carbonate was observed, a small but significant quantity of carbon dioxide was still noted in the fired product. The evolution of hydroxyl water from the dehydrate II phase is also indicated by these data. Correspondingly, a large endotherm can be seen in the DTA pattern at about 400° C., as well as a large weight-loss in the TGA pattern, at about 380° C. Thus the results of both the dynamic and static heating experiments suggest that water and carbon dioxide are evolved at about 320° C., yielding an oxide product.

A schematic representation of the thermal decomposition of coalingite is shown in Fig. 6. A cursory examination of the thermal decomposition of hydrotalcite indicates similar reactions. At about 150° C., hydrotalcite also dehydrates in a reversible manner.

GENESIS OF COALINGITE

In general, the Coalinga asbestos ore consists of a mixture of several physically different types of serpentine material including (1) hard, dense, dark-colored serpentinite fragments, ranging in size from fractions of an inch to boxcar dimensions and which consist of either lizardite or antigorite, chrysotile, brucite and magnetite, (2) large, tough, leathery

sheets of matted chrysotile, which range up to several square feet in size, (3) small, brittle, bladed and platy pieces of green serpentine, ranging in size from fractions of an inch to several square inches, and which have been found to be pure chrysotile, and (4) soft, flexible, flaky agglomerates of friable asbestos, varying from about $\frac{1}{4}''$ to $1''$ in diameter, and which contain appreciable amounts of both the hard serpentinite fragments and the green-bladed material. Although smaller amounts of brucite, magnetite and platy serpentine minerals are also present in this latter material, it consists predominantly of chrysotile itself.

From a study of numerous drill hole samples and hand specimens from various portions of the serpentinite, several pertinent observations have been made. Although the fresh asbestos ore, collected at depth, is gray-green in color, ore from the surface weathering zone is tan to gray-brown in color. Secondly, fresh ore is relatively rich in brucite, while surface ore is depleted in that phase and contains varying amounts of coalingite and the hydrotalcite-pyroaurite mineral discussed above. More specifically, the serpentinite "boulders" in the fresh ore appear to be enriched in brucite, compared with the softer asbestos surrounding them. Likewise, coalingite appears to be most abundant in the weathered "boulders" in the surface zone, which themselves are nearly devoid of brucite. Such observations by themselves suggest that coalingite is formed by the alteration of pre-existing brucite during the weathering of the Coalinga asbestos ore.

Petrographic studies of a number of the serpentinite "boulders" have shown that brucite is intimately associated with serpentine on a microscopic scale, probably the result of the original alteration of an olivine-rich rock to serpentine and brucite. Thin sections of both the hard, dense relatively unweathered inner portion of a large serpentinite "boulder," and of the softer, brown-colored, highly weathered outer portion of the same "boulder" were examined and are shown in Figs. 7 and 8. In the fresh, unweathered inner portion of the "boulder" brucite is present not only as vein fillings, but as scaly, randomly oriented aggregates admixed with the serpentine. The weathered, outer portion of the "boulder," shown in Fig. 8, contains abundant reddish-brown coalingite, filling veinlets, interspersed with brucite grains and intergrown with both the brucite and the serpentine. Although black and white prints only, are shown in Figs. 7 and 8, under crossed polars the light yellow color of brucite and the reddish brown color of coalingite readily distinguish these phases from the blue-white matrix of serpentine. These results corroborate the above suggestion that coalingite has formed from brucite in the surface weathering zone of the ore body.

Approximately twelve months after the sample from the inner, weathered portion of the serpentinite "boulder," described above, was identi-

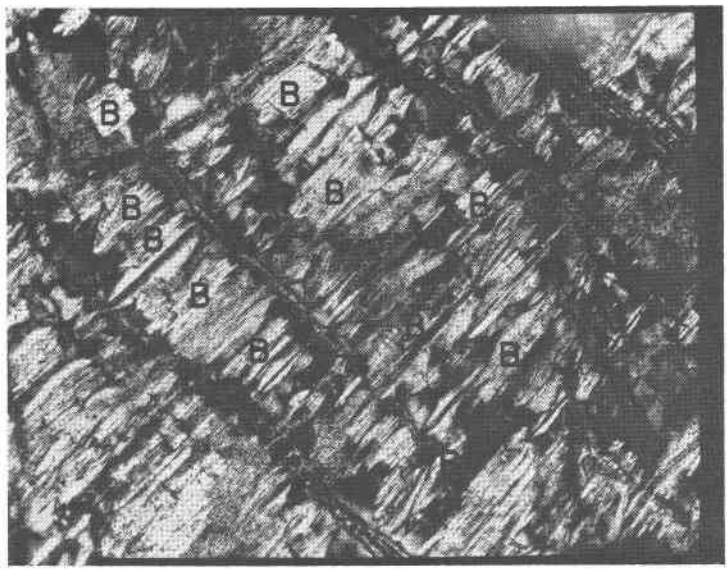

FIG. 7. Photomicrograph of fresh, unweathered, inner portion of a serpentinite "boulder." Brucite (B) in a matrix of serpentine. (Crossed polars, 150×).

fied by x-ray diffraction techniques as containing serpentine+brucite, a second examination of the same powdered sample was made. At this time the sample was found to consist of serpentine+some brucite+some coalingite. The surface of still another serpentinite sample was observed to have changed from a gray-green color to a mottled gray-brown color during this same period, and x-ray diffraction studies of material scraped from the discolored surface indicate the presence of a trace quantity of coalingite, which formed during the twelve-month exposure to the atmosphere. Such results strongly indicate that coalingite is formed from pre-existing brucite in air, and in a matter of months.

Electron probe analyses, using an Associated Electrical Industries apparatus, of a series of brucite-rich serpentinites from the New Idria serpentinite have indicated that much of the brucite present in the asbestos ore is significantly richer in iron than the serpentine material surrounding it. Typical data determined on a sample containing serpentine, brucite and magnetite, are discussed below and illustrated in Fig. 9. In Fig. 9A the electron image of the field examined is shown and an array of light and dark areas can be seen throughout the field. Such an assemblage is not atypical of the serpentinite specimens from this deposit examined to date and probably represents an intergrowth of serpentine and brucite (see also Fig. 7). The black grain in the upper right-hand corner of the field is magnetite. The silicon x-ray image, shown in Fig. 9B,

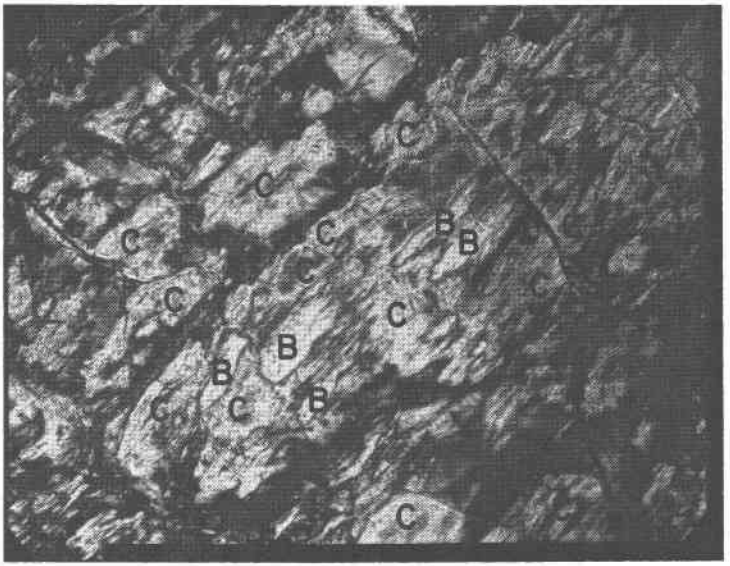

FIG. 8. Photomicrograph of friable, weathered portion of the same serpentinite "boulder" shown in Fig. 7. Coalingite (C) replacing brucite (B) in a matrix of serpentine (dark areas). (Crossed polars, 150×).

suggests that several regions of the field are devoid of silicon, while several others are substantially depleted in this element. The silicon-rich areas are undoubtedly serpentine. The magnetite grain is also free of silicon, as expected.

The magnesium x-ray image in Fig. 9C shows that, with the exception of the magnetite grain, magnesium is a ubiquitous constituent of the sample, and that it is present in about the same amount throughout. The iron x-ray image shown in Fig. 9D indicates that the silicon-free areas (brucite) are richer in iron than the surrounding serpentine material. A profile of the iron content across the field is shown in Fig. 9E superimposed on the electron image. The darker colored areas can be seen to be iron-rich. Quantitative estimates of the iron content of various points in the field by Mrs. G. Faulring are also listed in Fig. 9. From the data obtained on this sample and on several other similar samples, much of the brucite in the Coalinga asbestos deposit appears to contain about 15–18% iron.

These data, coupled with the brucite-coalingite transformations discussed above, indicate that coalingite develops directly from iron-rich brucite in serpentinite rocks of the Coalinga asbestos deposit in the surface oxidation zone of the deposit. In air, the following reaction is conceivable:

$$(Mg_{10}Fe_2^{2+})(OH)_{24} + 1/2O_2 + CO_2 + 2H_2O = Mg_{10}Fe_2^{3+}(CO_3)(OH)_{24}\cdot 2H_2O$$

Iron-rich brucite + air = coalingite

A similar reaction may also take place in the presence of carbon dioxide-rich ground waters, if the oxygen activity is high enough.

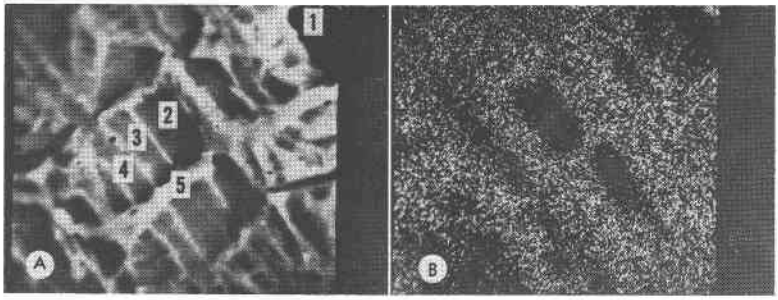

9A. Electron image

9B. Silicon x-ray image

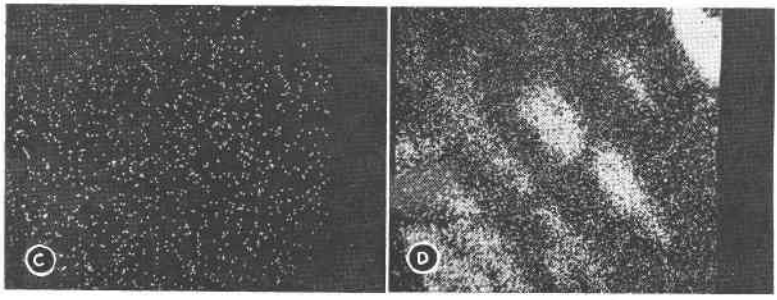

9C. Magnesium x-ray image

9D. Iron x-ray image

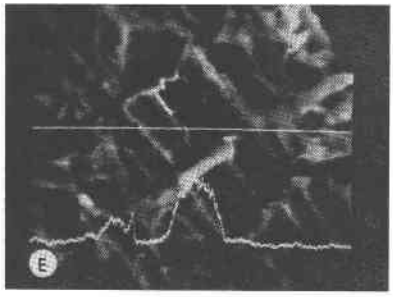

9E. Iron profile superimposed on electron image

Iron content at points indicated on the electron image (9A)

1 = 72% Fe
2 = 17.5%
3 = 2.2%
4 = 7.1%
5 = 1.8%

FIG. 9. Electron probe analysis of sample 487-52-7. Brucite-rich serpentinite from the Atlas pit. 360×.

ACKNOWLEDGMENTS

The authors are indebted to a number of individuals who contributed in various ways towards this investigation, including Mrs. G. Faulring who performed the electron probe calculations and carried out preliminary single crystal studies, W. K. Zwicker for many of the petrographic observations and to D. McLean, who carried out the semi-micro quantitative analyses. Thanks are also due to P. Pezzella and R. Brown for technical assistance in sample preparation operations, and to R. J. Kronkhyte, M. Genes and B. Mason for supplying samples of coalingite and related minerals for study. The authors' gratitude is also extended to R. G. Coleman, P. B. Hostetler, Michael Fleischer and Brian Mason for their counsel in this work, although they are not responsible for any errors of fact or interpretation contained herein.

REFERENCES

ABOVYAN, S. B. (1957) On new minerals from Armenia, associated with ultra-basic intrusive rocks. *Izvest. Akad. Nauk Armyan S.S.R., Ser. Geol.* **10** (4), 47–56.

Coleman, R. G. (1957) Mineralogy and petrology of the New Idria District, California. Ph.D. Thesis, Stanford Univ. (Univ. Microfilms Pub. 21, 566).

ECKEL, E. G. AND W. B. MYERS (1946) Quicksilver deposits of the New Idria District, San Benito and Fresno Counties, California. *Calif. Jour. Mines Geol.* **42,** Pt. 2, 81–124.

ELLSWORTH, H. V. (1939) Transparent green pyroaurite from Ontario. *Univ. Toronto Studies, Geol. Ser.* **42,** 33–45.

FENOGLIO, M. (1938) Richerche sulla brugnatellite. *Periodico Mineral.* **9,** 1–13.

FRONDEL, C. (1941) Constitution and polymorphism of the pyroaurite and sjögrenite groups. *Am. Mineral.* **26,** 295–315.

GINZBURG, I. I. AND I. A. RUKAVISHNIKOVA (1951) Minerals of the ancient crust of weathering of the Urals. *Akad. Nauk S.S.S.R. Inst. Geol. Nauk, Moscow,* 210–213.

LARSEN, E. S. AND H. BERMAN (1934) The microscopic determination of the nonopaque minerals. *U. S. Geol. Survey Bull.* **848,** 70.

MEIXNER, H. (1937) Artinit, Pyroaurit und Hydromagnesit aus Südserbien. *Zentr. Mineral. Abt. A,* 363–373.

MILLER, W. B. (1952) Asbestos in Yugoslavia, Part 2. *Asbestos* **34** (3), 2–10.

MUNRO, R. D. AND K. M. REIM (1962) Coalinga asbestos fiber, a newcomer to the asbestos industry. *Canad. Min. Jour.* **83,** 45–50.

PAVLOVIC, S. (1953) Asbestos deposits in Yugoslavia. *Bull. Scient. Conseil Acad. R.P.F. Yugo.* 1 (1), 15.

RICE, S. J. (1963) California asbestos industry. *Calif. Divis. Mines Geol. Mineral Infor. Ser.* **16** (9), 1–7.

SABINA, A. P. AND R. J. TRAILL (1960) Catalogue of *x*-ray diffraction patterns and specimen mounts at the Geological Survey of Canada. *Geol. Survey Canada Paper* **60-4,** 85.

SWANSON, H. E. *et al.* (1956) Standard *x*-ray diffraction patterns. *Natl. Bur. Stand. Circ.* **539,** vol. 6, 30.

Manuscript received, March 11, 1965; accepted for publication, June 18, 1965.